JOURNAL OF MATERIALS SCIENCE 27 (1992) 2231–2236

Micro-Raman spectroscopy study of the process of microindentation in polymers

Part I *Poly(3,3-dimethyl oxetane)*

T. JAWHARI, J.C. MERINO, J.M. PASTOR
Departamento Física de la Materia Condensada, Universidad de Valladolid, 47011 Valladolid, Spain

The residual deformation produced by Vickers microindentations in poly(3,3-dimethyl oxetane) (PDMO) was analysed by Raman microspectroscopy. Microstructural variations were observed as the Raman spectra were recorded at different positions along and out of the microindentation. A gradual distribution of the monoclinic and orthorhombic structures arises as the spectra were scanned from the centre to the edge of the impression area. This crystalline variation in PDMO, which reflects the degree of stress present on the surface of the sample, was utilized to obtain information on the distribution of pressure in and around the microindentation. In addition to the clear variation of pressure inside the permanently deformed region, no crystalline transformation was noted out of the impression area. Similar features were observed when the Raman spectra were recorded along one of the diagonals of the indentation.

1. Introduction

Microindentation techniques are routinely used in industry to test the resistance of the material to local deformation and to measure surface hardness. The microhardness technique basically consists in the impression of a microindenter of known geometry on the surface of the sample to study. Considering the concept of hardness, Tabor [1] differentiates between resistance to deformation during load and resistance to permanent deformation. Although the hardness value is defined as the resistance to deformation under load, the microhardness test usually measures the resistance to the plastic deformation produced by a load applied on a microindenter after having removed the load, which is given by the dimension of the residual impression. The size of the indentation being smaller than a few hundred micrometres, this technique is then considered as a non-destructive method.

Although the indentation hardness test is one of the oldest and one of the most widely utilized techniques for measuring the strength of materials, it remains one of the least fundamentally understood mechanical-analysis methods. The main reason for the lack of information about the process of deformation during the application of an indenter in a material is the difficulty of detecting experimentally the effects of the process of microindentation inside and around the impression.

Different models [2–7] have been proposed to describe the process of microindentation. Since the mechanisms of microindentation depend on the nature of the material, some of the theoretical models proposed fit well with the experimental results obtained in some types of material but not in others. The slip-line approach [2], which is based on the supposition that the indenter cuts the sample, is valid for ideal rigid–plastic materials, i.e. materials that are perfectly rigid up to a yield stress and then deform plastically without work-hardening. However, in the case of elastoplastic materials, this model shows some experimental inadequacies when the wedge angle of the indenter is greater than about 60° [3]. Mulhearn [3] developed the radial compression model to describe the process of microindentation by blunt indenters in metals. According to this model, deformation of the sample occurs by radial compression of hemispherical shells centred at the point of first contact, with the magnitude of the strains diminishing as the elastic–plastic boundary is approached. More recently Loubet *et al.* [5] proposed a model for Vickers indentation in elastoplastic materials. This model still considers the two zones, i.e. the plastically deformed region and the elastically deformed zone out of the impression area which is characterized by an elastic deflection of the material surface occurring during load at the edge of the plastically deformed zone.

On the other hand, microhardness techniques have been little and hesitantly applied in the field of polymer science. The reason for this is the complex viscoelastic deformation behaviour of polymeric materials. It is often difficult to obtain consistent microhardness data on polymers because of creep that may occur under load and a time-dependent recovery when the load is removed.

Furthermore, the description of the process of microindentation in semicrystalline polymers is complicated by the different phases of the material, i.e. the crystalline region, the interface and the amorphous

0022–2461

part. Some workers [8–11] have attempted to correlate the microhardness of polyethylene with its structure (lamellar thickness, crystallinity, orientation etc.) and found that the microhardness value is a property which is related to the thickness of crystalline lamellae. Other workers [12–16] have shown clear variations of the microhardness value below and above the glass transition temperature. The mechanism of microindentation in semicrystalline polymers is a complex process that depends on the viscoelastic properties of polymers such as creep and time-dependent degree of recovery, which are influenced by the degree of crystallinity, lamellar thickness, etc.

Although the mechanisms of the microindentation process in polymers are still unclear, the microhardness technique is more and more frequently utilized since the method is relatively simple, non-destructive and can provide rapid information on the mechanical properties at the surface of the specimen. This technique is also used for its high sensitivity to detect second-order transitions [12–16] or phase transitions [17].

The aim of this work is to improve the present knowledge of the process of microindentation in polymers. To date the mechanisms of deformation by microindentation have not been analysed at a molecular level. In this study we shall investigate molecular structural variation in the microindentation region in order to obtain information on the stress distribution. For this purpose, it was decided to use an experimental technique that gives information on the molecular level and can be combined with the microindentation method. It was also necessary to choose a sample that shows clear structural variations with pressure which can be analysed by the method utilized. To analyse microstructural changes the micro-Raman technique was used for the different advantages that it offers: it can be easily utilized to examine the zone deformed by the microhardness test; it has a spatial resolution of the order of 1–2 μm as will be shown below; it is sensitive to conformational variation; and it allows the study of materials with no preparation or alteration of the sample.

The sample chosen was poly(3,3-dimethyl oxetane) (PDMO) since it was previously shown [18] that the ratio between its crystalline structures depends on the pressure applied to the specimen. This dependency will then be utilized to obtain information on the distribution of stress in the microindentation.

2. Experimental procedure

2.1. Materials

In previous studies [19–21], it was shown that PDMO presents different crystalline structures that are sensitive to thermal effects and/or mechanical deformation processes. The crystallization of PDMO from the melt state at a crystallization temperature superior to 16 °C will only produce the monoclinic structure (form II) with a conformation $T_3GT_3\bar{G}$, whereas at a crystallization temperature below 0 °C the orthorhombic structure (form III) with a conformation $(T_2G_2)_2$ is formed. When PDMO is crystallized between 0 °C and 16 °C the two crystalline structures are present.

The PDMO samples utilized during this study were described previously [20]. In this work, two series of PDMO samples were analysed:

(i) Sample A was cooled from the melt and then annealed at −16 °C for 10 h in order to obtain a crystalline phase principally composed of structure III.

(ii) Other samples B and C were then prepared by pressing sample A at room temperature under 400 and 700 bar, respectively.

(iii) Sample D was crystallized at room temperature and then annealed at 45 °C for 14 h; its Raman spectrum only exhibits the bands characteristic of structure II.

2.2. Testing procedures

A Vickers microhardness instrument (square pyramidal diamond indenter with an apical angle of 136°) combined with an optical universal Zeiss microscope was utilized during this work. The indentations were made at room temperature and the loads were applied for approximately 30 s.

The micro-Raman instrument utilized was a multichannel detection (512 intensified diodes) Dilor XY spectrometer using as the dispersive system a foremonochromator (a double monochromator) followed by a spectrograph. The Raman instrument was combined with a standard Olympus microscope which allows the Raman analysis of microsample with a precision of the order of 1–2 μm, as will be demonstrated in the next section. The spectra were all recorded with a spectral bandpass of 150 μm and the corresponding resolution was 3 cm^{-1}. The 514.5 nm line of a Spectra Physics argon-ion laser (model 2020/5w) was used as the excitation source. The laser power at the sample position was 20 mW. An acquisition time of 3 s was used and the number of acquisitions was either 25 or 50 depending on the quality of the Raman signal obtained.

3. Results

3.1. Spatial resolution

Most of the manufacturers of micro-Raman spectrometers give a theoretical value for the spatial resolution of 1 μm or even less, which is usually the diffraction-limited spatial resolution. During this study, it was decided to check whether or not this theoretical value is deteriorated by optical components or any excessive scattering effect from the sample. For this a thin layer of silver was vacuum-deposited on to a polymer film and Raman spectra were recorded at different positions across the polyethylene–silver interface. The Raman spectra were obtained by positioning the polyethylene–silver sample on a microscope translation stage controlled by a computer and driven by a stepper-motor allowing xy displacements of 0.25 μm. Fig. 1 shows the variation of the Raman intensity of the polyethylene band at 2884 cm^{-1} as the laser source position is

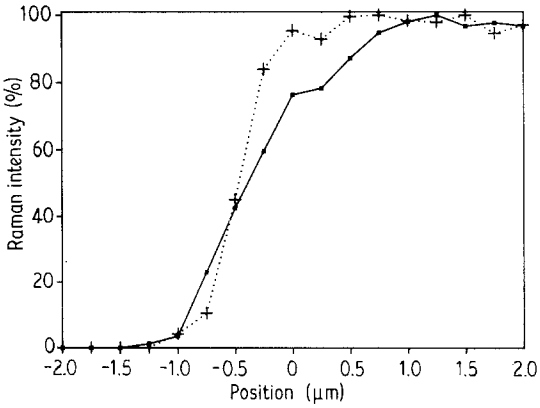

Figure 1 Raman intensity of the polyethylene band at 2884 cm^{-1} against the position across the polyethylene–silver interface. The position 0 μm corresponds to the interface. (+) Spectrum recorded with pinhole, (■) spectrum recorded without pinhole.

scanned across the interface. It can be observed that for routine work the spatial resolution is of the order of 2 μm, and that this can be improved to approximately 1 μm by using a 400 μm diameter pinhole situated at an intermediate image plane before the entrance of the spectrometer.

3.2. Micro-Raman analysis

In a previous study [18], we observed that PDMO shows a gradual crystalline variation from structure III to II as the pressure applied to the sample is increased. This crystalline variation was best observed in the vibrational region between 800 and 830 cm^{-1} which corresponds to the breathing mode in PDMO [22]. Three Raman bands are present in this vibrational domain at 804, 815 and 822 cm^{-1} and were assigned to the monoclinic structure, amorphous region and orthorhombic structure, respectively.

Fig. 2 represents a photograph of a microindentation obtained on PDMO. In this study, the Raman spectra were scanned along two directions, i.e. along the diagonal of the indentation and the line of maximum gradient in depth (see Fig. 2). The points which are illustrated indicate the different positions where the Raman spectra were recorded. The centre of the indentation will be considered as the origin of the two axes formed by the diagonals of the indentation.

Fig. 3 shows four Raman spectra of sample A recorded in the centre of the indentation (position A) and at the positions B (10 μm, 10 μm), C (20 μm, 20 μm) and D (30 μm, 30 μm). Similarly, Fig. 4 illustrates the variation of the Raman spectrum along one of the diagonals produced by the sharp edge of the indenter at positions A (centre), E (0 μm, 10 μm), F (0 μm, 20 μm) and G (0 μm, 50 μm).

Fig. 5 gives two Raman spectra of sample D, one recorded in the centre of the indentation and the other out of the impression.

Similarly to Fig. 3, Figs 6 and 7 illustrate the variation of the Raman spectra along the microindentation obtained in samples B and C.

Table I shows the percentage of the two crystalline structures, II and III, and amorphous region for the four Raman spectra presented in Fig. 3. The percentages of each phase were calculated by measuring the areas of the three bands, appearing between 800 and 830 cm^{-1} and characteristic of the three different structures, after deconvolution of these three Raman bands. An example of an original spectrum corresponding to the breathing-mode region of PDMO with its deconvoluted counterpart is illustrated in Fig. 8.

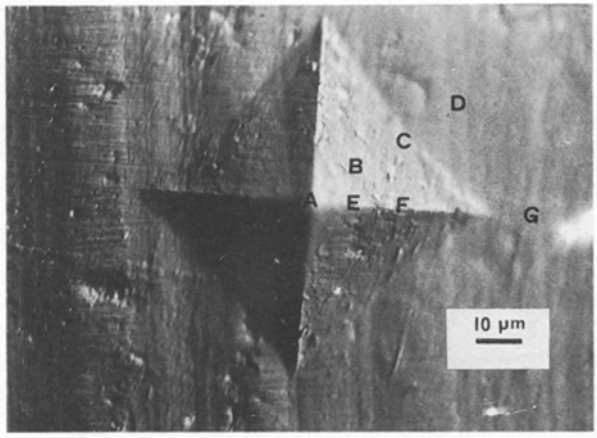

Figure 2 Photograph of a microindentation obtained on PDMO. The diagonal length and load were 80 μm and 200 mN, respectively. The Raman spectra were recorded along the line of maximum gradient in depth at the positions A (centre of the indentation), B (10 μm, 10 μm), C (20 μm, 20 μm) and D (30 μm, 30 μm) and along the diagonal at the positions A, E (0 μm, 10 μm), F (0 μm, 20 μm) and G (0 μm, 50 μm).

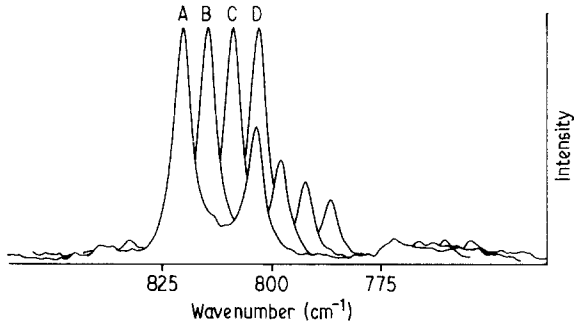

Figure 3 Raman spectra recorded along the microindentation made in sample A at the positions A, B, C and D.

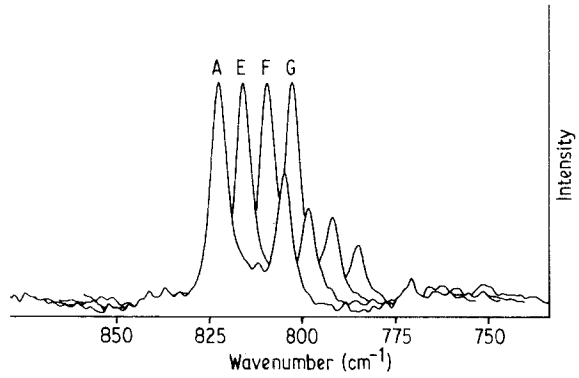

Figure 4 Raman spectra of sample A recorded at the positions A, E, F and G.

4. Discussion

Figs 3, 4, 6 and 7 show clear changes in the Raman spectrum of PDMO characteristic of the breathing

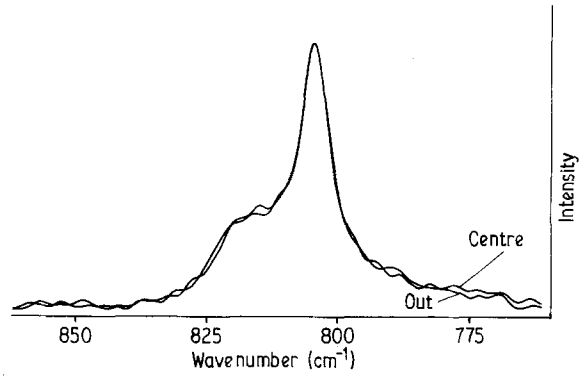

Figure 5 Raman spectra of sample D recorded in the centre of the indentation and out of the impression area.

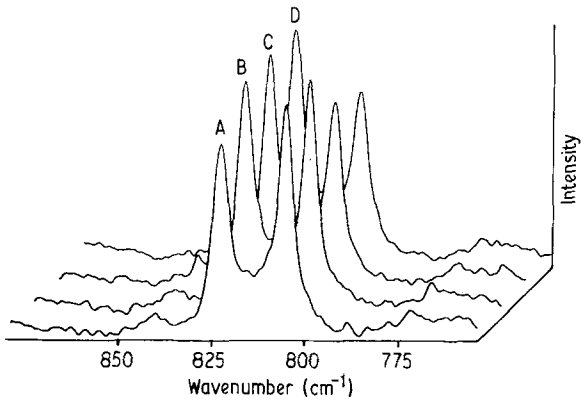

Figure 6 Raman spectra of sample B recorded at the positions A, B, C and D.

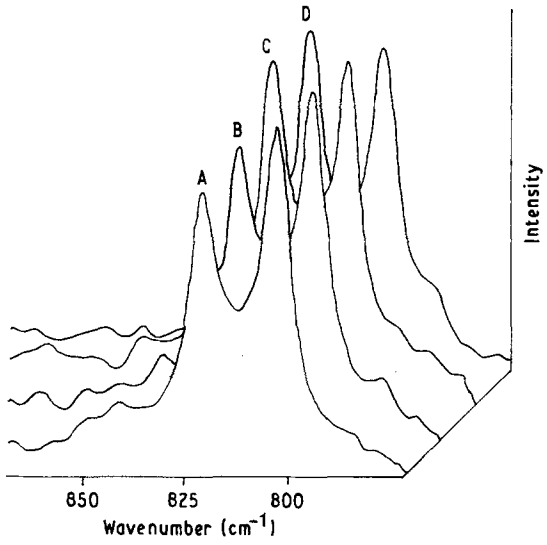

Figure 7 Raman spectra of sample C recorded at the positions A, B, C and D.

TABLE I Area percentage of the three Raman bands corresponding to structure II, structure III and the amorphous region of PDMO versus the position of the recorded spectra

Analysed position	Structure II (%)	Structure III (%)	Amorphous region (%)
A (0 μm, 0 μm)	30	52	18
B (10 μm, 10 μm)	24	56	20
C (20 μm, 20 μm)	19	63	18
D (40 μm, 40 μm)	14	66	20

mode as the analysed position along the indentation is varied from the edge to the centre. As the analysed position gets closer to the centre of the indentation, the intensity of the 822 cm^{-1} band diminishes whereas that of the 804 cm^{-1} band increases. Table I indicates that these variations in the Raman intensity corresponds to a transformation in the crystalline structure from structure III to II, with no significant variation in the extent of the amorphous phase. On the other hand, Fig. 5 shows that the indentation obtained on a sample containing only structure II does not produce any crystalline transformation from structure II to III. Thus, only the variation III to II can be produced by pressure in PDMO. All these results are in good agreement with previous work [18–22].

Comparing Figs 6 and 7 with Fig. 3, it can be observed that an indentation made on a sample that was already partially transformed to structure II will still produce an additional crystalline transition from form III to form II, and as a result will increase the amount of structure II in the impression area.

Similar spectral features were noticed when the Raman spectra were recorded at different positions along the diagonal produced by the sharp edge of the indenter (see Fig. 4). Thus, the mechanism of deformation produced by the sharp edge of the indenter seems to be similar to that due to the faces of the pyramidal indenter. Thus, as expected, the microindentation made in a polymer by a blunt indenter does not produce a cutting process in the material.

No significant crystalline variation could be observed when the Raman spectrum of PDMO was recorded out of the impression zone, whereas at the contact zone between the indenter and the polymer a crystalline transition was detected. This observation is in good agreement with the model proposed by Loubet *et al.* [5] to describe the microindentation process in elastoplastic materials; inside the indented zone, plastic deformation occurs whereas outside the impression the deformation process is elastic. This is a simple model that combines both elastic and plastic behaviours of the material. This is illustrated in Fig. 9, which represents the process of microindentation under load with the two separate zones, i.e. elastic displacement outside the area of contact and plastic displacement inside the impression.

In the contact zone during the process of microindentation, the distribution of pressure is not known analytically; it is usually considered roughly uniform [23]. This is valid for the case where the process of microindentation follows the mechanisms of deformation in ideal rigid–plastic materials where the shape of the impression stays undisturbed after formation of the indentation. In previous work [18] we showed that a clear dependency exists between the pressure applied to PDMO and its degree of crystalline transformation from structure III to II. The results that we present here indicate that the crystalline transition from structure III to II is not constant along the indentation, i.e. the transformation is greater at the centre than at the edge of the indentation. This variation in the crystalline structure reflects the distribution of tension inside the microindentation. The gradient in

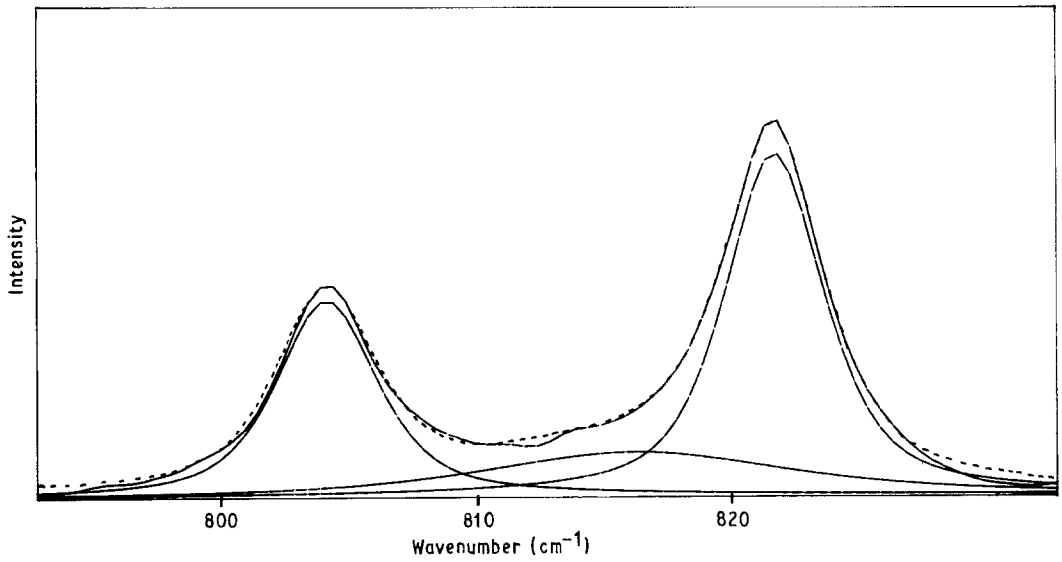

Figure 8 (——) Original spectrum of PDMO between 790 and 830 cm^{-1} with its deconvoluted counterparts; (– – –) the calculated fit.

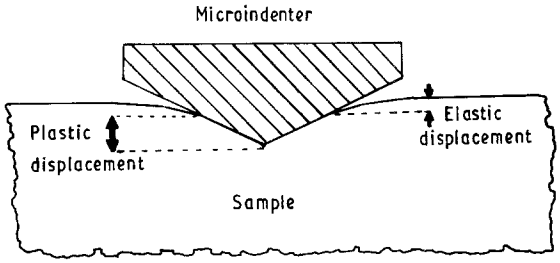

Figure 9 Schematic diagram showing the process of microindentation during load.

the pressure distribution experimentally observed may be explained by different features of the process of microindentation in polymers:

(i) The degree of elastic deflection which surrounds the contact zone as described in Fig. 9 will vary as the indenter penetrates the sample. This will result in a variation of the elastic forces occurring during the loading process which may affect the distribution of pressure inside the contact zone.

(ii) It is probable that at the centre and around the centre, a region of high strain (similar to the high-strain metal cap proposed by Mulhearn [3] in his compression model for metals) grows as it advances within the sample during loading. A type of work-hardening around the tip of the indenter would consequently occur during the process of indentation, producing a variation in the distribution of pressure inside the deformed zone.

(iii) It is known that the process of microindentation in polymers is associated with the mechanism of creep. The degree of creep may vary during the loading of the microindenter due to the expansion of the high-strain cap around the centre of the indenter. As a result this may affect the pressure distribution along the indentation.

5. Conclusions

This present study, which is the first direct molecular analysis inside and outside the microindentation, has brought out some new interesting aspects in the description of the deformation process on the surface of semicrystalline polymers due to a Vickers microindentation. Out of the contact area, no crystalline phase transition was detected. This agrees well with the model proposed for elastoplastic material, where out of the indentation the deformation is elastic with total recovery after removing the load. This work also shows that the distribution of pressure along the impression is not constant; it is greater in the centre and falls off as the position reaches the edge of the indentation.

The method presented in this work, which is based on the correlation between the degree of crystalline transformation and the pressure, appears to be an interesting approach to obtaining information on the distribution of stress inside a micro-region.

Acknowledgements

The authors are grateful to the Junta de Castilla y León and CICYT under the project PA86-0198 for financial support.

References

1. D. TABOR, "The Hardness of Metals" (Clarendon, Oxford, 1951) p. 112.
2. R. HILL, E. H. LEE and S. J. TUPPER, *Proc. R. Soc.* **A188** (1947) 273.
3. T. O. MULHEARN, *J. Mech. Phys. Solids* **7** (1959) 85.
4. M. C. SHAW and J. G. De SALVO, *Trans. Amer. Soc. Mech. Engng* **B92** (1970) 480.
5. J. L. LOUBET, J. M. GEORGES and G. MEILLE, in "Microindentation Techniques in Materials Science and Engineering", edited by P. J. Blau and B. R. Lawn (ASTM, Philadelphia, 1986) p. 72.
6. L. E. SAMUELS, *ibid.* p. 5.
7. D. TABOR, *ibid.* p. 129.
8. F. J. BALTA-CALLEJA, J. MARTINEZ-SALAZAR, H. CACKOVIC and J. LOBODA-CACKOVIK, *J. Mater. Sci.* **16** (1981) 739.
9. F. J. BALTA-CALLEJA, *Adv. Polym. Sci.* **66** (1985) 19.
10. F. J. BALTA-CALLEJA and H.-G. KILIAN, *Coll. Polym. Sci.* **266** (1988) 29.
11. V. LORENZO, J. M. PEREÑA and J. G. FATOU, *Angew. Makromol. Chem.* **172** (1989) 25.

12. J. M. PASTOR, A. GONZÁLEZ and J. A. SAJA, *J. Appl. Polym. Sci.* **38** (1989) 2283.
13. B. MARTIN, J. M. PEREÑA, J. M. PASTOR and J. A. SAJA, *J. Mater. Sci. Lett.* **5** (1986) 1027.
14. F. ANIA, J. MARTINEZ-SALAZAR and F. J. BALTA-CALLEJA, *J. Mater. Sci.* **24** (1989) 2934.
15. J. M. PEREÑA, B. MARTIN and J. M. PASTOR, *J. Mater. Sci. Lett.* **8** (1989) 349.
16. C. C. GONZALEZ, J. M. PEREÑA, A. BELLO, B. MARTIN, J. C. MERINO and J. M. PASTOR, *ibid.* **8** (1989) 1418.
17. J. MARTINEZ-SALAZAR, J. C. CANALDA CAMARA, E. LÓPEZ CABARCOS, F. J. BALTÁ-CALLEJA and H.-G. KILIAN, *Coll. Polym. Sci.* **266** (1988) 41.
18. J. C. MERINO, J. M. PASTOR, A. De SAJA and D. CHRISTEN, *J. Mol. Struct.* **143** (1986) 183.
19. Y. TAKAHASHI, Y. OSAKI and H. TADAKORO, *J. Polym. Sci., Polym. Phys. Edn* **18** (1980) 1863.
20. J. C. MERINO, J. M. PASTOR, A. De SAJA, E. PÉREZ, J. G. FATOU, A. BELLO and J. G. FATOU, *Eur. Polym. J.* **21** (1985) 449.
21. E. PÉREZ, J. G. FATOU, A. BELLO, J. C. MERINO, J. M. PASTOR and A. De SAJA, *Makromol. Chem.* **186** (1985) 1731.
22. J. C. MERINO, J. M. PASTOR, A. De SAJA and D. CHRISTEN, *Polymer* **29** (1988) 661.
23. N. A. STILWELL and D. TABOR, *Proc. Phys. Soc.* **78** (1961) 169.

Received 10 December 1990
and accepted 13 May 1991